



South Asian river basins in a 1.5 °C warmer world

Arthur F. Lutz¹ · Herbert W. ter Maat² · René R. Wijngaard^{1,3} · Hester Biemans⁴ · Abu Syed⁵ · Arun B. Shrestha⁶ · Philippus Wester⁶ · Walter W. Immerzeel^{1,3}

Received: 22 October 2017 / Accepted: 21 October 2018 / Published online: 19 November 2018
© The Author(s) 2018

Abstract

In 2015, with the signing of the “Paris Agreement”, 195 countries committed to limiting the increase in global temperature to less than 2 °C with respect to pre-industrial levels and to aim at limiting the increase to 1.5 °C by 2100. The regional ramifications of those thresholds remain however largely unknown and variability in the magnitude of change and the associated impacts are yet to be quantified. We provide a regional quantitative assessment of the impacts of a 1.5 versus a 2 °C global warming for a major global climate change hotspot: the Indus, Ganges, and Brahmaputra river basins (IGB) in South Asia, by analyzing changes in climate change indicators based on 1.5 and 2 °C global warming scenarios. In the analyzed ensemble of general circulation models, a global temperature increase of 1.5 °C implies a temperature increase of 1.4–2.6 ($\mu = 2.1$) °C for the IGB. For the 2.0 °C scenario, the increase would be 2.0–3.4 ($\mu = 2.7$) °C. We show that climate change impacts are more adverse under 2 °C versus 1.5 °C warming and that changes in the indicators’ values are in general linearly correlated to average temperature increase. We also show that for climate projections following Representative Concentration Pathways 4.5 and 8.5, which may be more realistic, the regional temperature increases and changes in climate change indicators are much stronger than for the 1.5 and 2 °C scenarios.

Keywords Climate change · 1.5 degrees · South Asia · Indus · Ganges · Brahmaputra · Paris agreement

Editor: Erika Coppola.

Electronic supplementary material The online version of this article (<https://doi.org/10.1007/s10113-018-1433-4>) contains supplementary material, which is available to authorized users.

✉ Arthur F. Lutz
a.lutz@futurewater.nl

Herbert W. ter Maat
h.termaat@enschede.nl

René R. Wijngaard
r.r.wijngaard.uu@gmail.com

Hester Biemans
hester.biemans@wur.nl

Abu Syed
abu.syed@bcas.net

Arun B. Shrestha
arun.shrestha@icimod.org

Philippus Wester
philippus.wester@icimod.org

Walter W. Immerzeel
w.immerzeel@futurewater.nl

¹ FutureWater, Costerweg 1V, 6702 AA Wageningen, The Netherlands

² Municipality of Enschede, Enschede, The Netherlands

³ Department of Physical Geography, Utrecht University, Utrecht, The Netherlands

⁴ Wageningen Environmental Research, Wageningen, The Netherlands

⁵ Bangladesh Centre for Advanced Studies, Dhaka, Bangladesh

⁶ International Centre for Integrated Mountain Development, Kathmandu, Nepal

Introduction

Climate change is identified as one of the major global issues, threatening the planet at various levels (IPCC 2014). Multiple attempts to streamline global policy on climate change mitigation have been made over the past decades, and the “Paris Agreement” which was signed at the 21st Conference of the Parties in 2015 is considered a major breakthrough in formulating adequate measures to tackle climate change (Clemencon 2016; Savaresi 2016). During that conference, 195 countries agreed on “a long-term goal of keeping the increase in global average temperature to well below 2 °C above pre-industrial levels,” and “to aim to limit the increase to 1.5 °C, since this would significantly reduce risks and the impacts of climate change.” In response to this development, the Intergovernmental Panel on Climate Change (IPCC) has published a Special Report on global warming of 1.5 °C above pre-industrial levels (IPCC 2018). However, scientific evidence of the impacts of a 1.5 °C global warming, and the differences in impacts between 1.5 °C and a 2 °C global warming, is still sparse. Therefore, the scientific community has been mobilized to provide this scientific evidence (NCC 2016). A global study of differences in impacts at 1.5 and 2.0 °C forms a starting point for such assessments and highlights the importance of regional differentiation (Schleussner et al. 2016b). The aim of our study is to provide a regional quantitative assessment of the impacts of a 1.5 °C versus a 2 °C global warming for a major global climate change hotspot: the Indus, Ganges, and Brahmaputra river basins in South Asia (De Souza et al. 2015).

Developing countries and their inhabitants are considered to be more vulnerable to climate change than western countries (Mertz et al. 2009). The glacier-fed Indus, Ganges, and Brahmaputra (IGB) river basins in South Asia are home to a population around 660 million people (Shrestha et al. 2015), which is projected to increase to almost 1 billion by 2050 (UN 2015). With the increasing population, demands for water, food, and energy will increase strongly too. The region is facing enormous challenges in adapting to climate change, which is impacting many different sectors, in addition to conventional development challenges that lead to adaptation deficits (Kilroy 2015; Vinke et al. 2017).

The regional climate is dominated by the Asian summer monsoon, protruding from the south-east to the north-west of the region, and bringing large amounts of precipitation during June to September. The largest amounts of precipitation fall close to the Bay of Bengal, and at the southern slopes of the Hindu-Kush-Himalayas where the steep rise in topography causes orographic precipitation (Galewsky 2009) (Fig. 1). Under climate change, changes in monsoon duration and intensity are expected (Turner and Annamalai 2012; Sperber et al. 2013), and over a historical period increases in dry and wet spells are observed during the monsoon season (Singh

et al. 2014). Increases in frequency and magnitude of heavy precipitation events will increase the occurrence of floods (Mirza 2011; Hirabayashi et al. 2013), river bank erosion, and other natural hazards like landslides, debris flows, and glacier-lake outburst floods (GLOFs) (Tariq et al. 2014). Besides, increases in precipitation intensity lead to increasing sedimentation, affecting hydropower production and the lifetime of hydropower infrastructure.

Droughts are expected to increase globally under climate change in combination with an increase in human water use (Trenberth et al. 2013; Wanders and Wada 2014). This affects agricultural production and therefore regional food security (Wheeler and von Braun 2013; Biemans et al. 2013), and may lead to insufficient flows to sustain ecosystem services, or the drying up of springs (Tambe et al. 2012). In the Indus and Ganges basins, large portions of irrigation water come from non-renewable groundwater already in the present situation (Gleeson et al. 2012; Gleeson and Wada 2013). Heat waves also affect agricultural production, can trigger GLOFs, and affect human health (Pal and Eltahir 2015), and are projected to be severe in South Asia (Im et al. 2017). Changes in temperature and humidity affect the transmissivity of vector-borne diseases like malaria (Dhiman et al. 2011).

The Indus, Ganges, and Brahmaputra rivers depend significantly on glacier and snow melt water (Immerzeel et al. 2010; Lutz et al. 2014), and climate change affects cryospheric water reserves stored in the Hindu-Kush, Karakoram, and Himalayan mountain ranges. Glaciers have been retreating in recent decades (Bolch et al. 2012; Brun et al. 2017), and ice masses will reduce further under climate change (Kraaijenbrink et al. 2017), with temperature increases being stronger at high altitude compared to lower land areas (Pepin et al. 2015; Palazzi et al. 2016). The changes in the cryosphere will lead to changes in downstream water availability, and timing and magnitude of flow (Lutz et al. 2016a).

The Ganges-Brahmaputra delta is additionally threatened by increases in flooding events related to the subsidence of land (Higgins et al. 2014), rising sea levels (Nicholls and Cazenave 2010; Kay et al. 2015), and increases in tropical cyclone activity over the Bay of Bengal during the postmonsoon season (Balaguru et al. 2014).

Many of these impacts can be directly linked to changes in air temperature and precipitation, or climate change indicators derived from those variables. The aim of this study is to provide a quantitative overview of the impacts of climate change for the 1.5 °C global warming scenario, the 2.0 °C global warming scenario, and an ensemble of downscaled region-representative climate projections for the end of the twenty-first century, under the Representative Concentration Pathways (van Vuuren

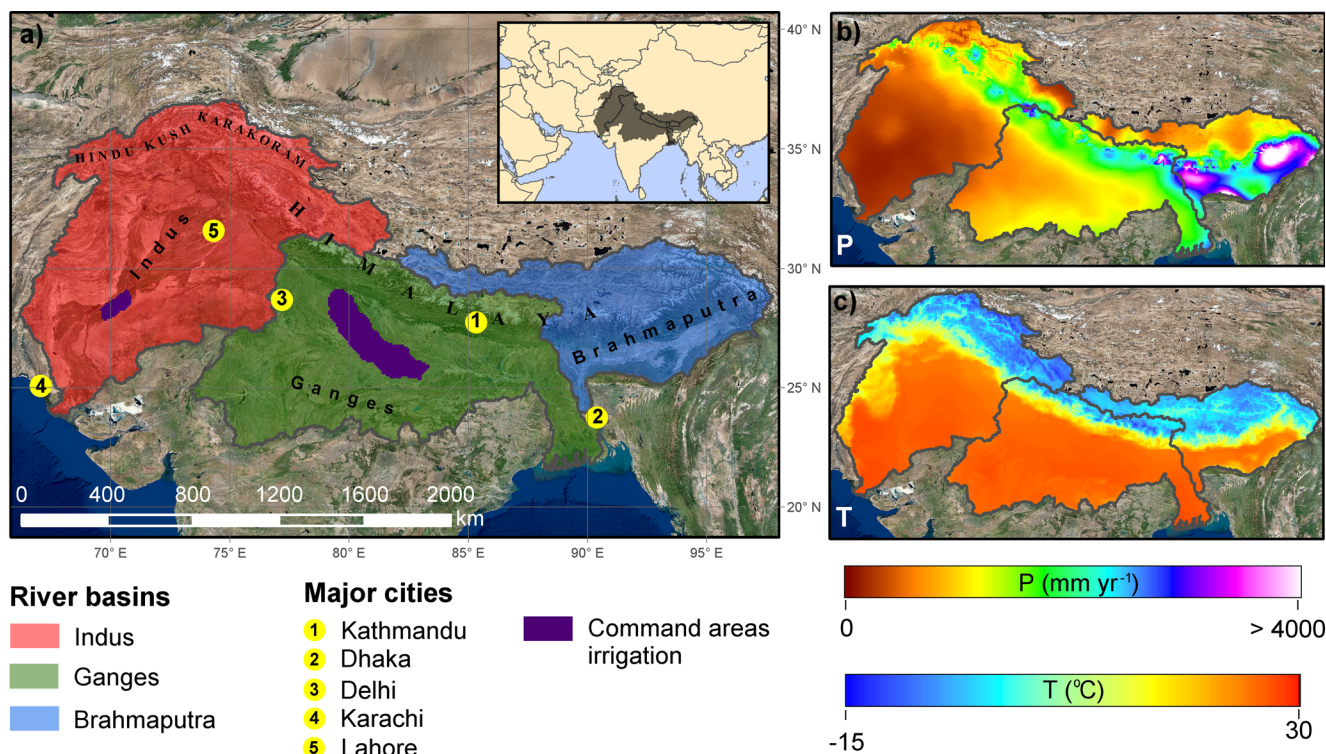


Fig. 1 a Study area. b Average annual precipitation for reference period (1981–2010, REF). c Average air temperature for reference period (1981–2010, REF)

et al. 2011) RCP4.5 and RCP8.5. To this end, we analyze a set of ten climate change indicators, which can be derived from changes in air temperature and precipitation, and compare these for the four scenarios (i.e., 1.5 °C, 2.0 °C, end of century RCP4.5 and end of century RCP8.5). The ten indicators are chosen in such a way that they can be directly or indirectly related to the most important sectors in the region.

Data and methods

Downscaled climate change scenarios

We use an ensemble of 2 × 4 downscaled general circulation models (GCMs), which is representative for the complete set of climate change projections under RCP4.5 and RCP8.5 in the Coupled Model Intercomparison Project Phase 5 (CMIP5) multi-model ensemble (Taylor et al. 2012), over the IGB region (Table 1). The GCMs have been selected in such a way that they reflect the full ranges of projected climate change in terms of changes in climatic means and climatic extremes. Besides, only climate models with sufficient skill in simulating historical climate in the region have been included in the ensemble (Lutz et al. 2016b). The eight selected GCMs’ outputs for precipitation, mean air temperature, maximum air temperature, and minimum air temperature have been

downscaled and bias corrected by applying the empirical-statistical quantile mapping method (e.g., Piani et al. 2010; Themeßl et al. 2011a), to the future GCM projections using a historical reference climate dataset for the IGB basins. This reference dataset covers 1981–2010 at a daily time step with a 10 × 10-km spatial resolution (Lutz and Immerzeel 2015). The downscaled GCMs cover 2011–2100 at the same time step and spatial resolution. The quantile mapping methodology is robust and well established, and has been proven to perform well over mountainous regions (Themeßl et al. 2011b; Immerzeel et al. 2013). It has been successfully applied for the Indus, Ganges, and Brahmaputra river basins before (Wijngaard et al. 2018). We follow the methodology described by Themeßl et al. (2011a). However, instead of calculating empirical cumulative distribution functions (ecdfs) for each day of the year, we construct ecdfs for each month of the year (moy, 12 months). We do this for each 10 × 10-km grid cell (i), from the daily values spanning 1981–2010 of the reference climate dataset (obs), which is based on observations.

For the historical GCM runs for 1981–2010, the same procedure is followed to generate ecdfs for each month of the year, after the GCM grids have been smoothed from their original spatial resolution to 10 × 10 km using a bilinear interpolation. Both sets of ecdfs (i.e., for the reference climate dataset (obs) and the historical GCM runs (GCM)) are used to construct a correction function (CF):

$$CF_{t,i} = \text{ecdf}_{\text{moy},i}^{\text{obs,ref}^{-1}}(P_{t,i}) - \text{ecdf}_{\text{moy},i}^{\text{GCM,ref}^{-1}}(P_{t,i})$$

where $P_{t,i}$ is the probability of a future GCM value, which is derived as:

$$P_{t,i} = \text{ecdf}_{\text{moy},i}^{\text{GCM,fut}^{-1}}(X_{t,i}^{\text{raw}})$$

The correction function CF is used to downscale and bias-correct the future GCM runs spanning 2011–2100 at a daily time step. For each day and each grid cell, this is done as follows:

$$Y_{t,i}^{\text{cor}} = X_{t,i}^{\text{raw}} + CF_{t,i}$$

Similar as described by Themeßl et al. (2011a), we include frequency adaptation, to account for cases where the dry-day frequency in the GCM is greater than in the observations, and the generation of new extremes by linear extrapolation of the correction value (CF) at the highest and lowest quantiles of the calibration range (i.e., the 1981–2010 reference period). See Themeßl et al. (2011a) for further details. In this way, transient gridded meteorological time series from 2011 to 2100 at 10×10 -km spatial resolution and daily time step are constructed for each of the selected GCM runs.

The quantile mapping is validated by a decadal “leave one out” cross-validation approach (e.g., Themeßl et al. 2011b, a). This is done by constructing the ecdfs for the reference climate dataset and historical GCM runs for 20 out of 30 years of the reference period (e.g., 1981–2000) and subsequently using those ecdfs and the derived correction function to downscale the historical GCM runs for the remaining 10 years of the

reference period (e.g., 2001–2010). This procedure is repeated to downscale the two remaining 10-year periods of the reference period: ecdfs for 1991–2010 are used to downscale 1981–1990 and ecdfs for 1981–1990 and 2001–2010 combined are used to downscale 1991–2000. The downscaled GCM data of precipitation for 1981–2010 is validated to the reference dataset, by comparing the mean precipitation, number of dry days, and 99th percentile value of precipitation. For air temperature, we validate the mean and 1st and 99th percentile values of mean, maximum, and minimum air temperature. This comparison is done for the entire distributions of daily values spanning 30 years covering 1981–2010. Because the reference dataset covers 27,164 grid cells, it is computationally not feasible to do this comparison for each individual grid cell. To overcome this, we do the comparison for 100 randomly sampled grid cells in each of the three river basins.

Extraction and analysis of GCM time slices of 1.5 and 2.0 °C global temperature increase with respect to the preindustrial era

Because of the large computational effort required for the bias-correction and downscaling described in the “Downscaled climate change scenarios” section, the downscaling has been limited to the IGB region, and the period 2011–2100 which is adjacent to the reference period (1981–2010). Since the 1.5 and 2 °C scenarios concern global averages, analyses comparing global and regional future climate to the preindustrial area were done using the raw (i.e., non-downscaled, at their original spatial resolutions) global daily grids of the eight selected GCM runs as available from the CMIP5 archive. We analyze the global temperature change by taking

Table 1 Analyzed GCM runs listing time slices for which global temperature changes (ΔT) of 1.5 and 2.0 °C compared to pre-industrial (PI) levels are reached, the corresponding regional changes in air temperature (ΔT IGB) and precipitation (ΔP IGB), and the projected

regional changes in air temperature (ΔT IGB EOC) and precipitation (ΔP IGB EOC), at the end of the 21st century (EOC 2071–2100), compared to pre-industrial levels

GCM run	Time slice 1.5 °C global increase vs. PI reached	ΔT IGB global 1.5 °C vs. PI [°C]	ΔP IGB global 1.5 °C vs. PI [%]	Time slice 2.0 °C global increase vs. PI reached	ΔT IGB global 2.0 °C vs. PI [°C]	ΔP IGB global 2.0 °C vs. PI [%]	ΔT IGB EOC vs. PI [°C]	ΔP IGB EOC vs. PI [%]
BNU-ESM_rcp45_r1i1p1	1994-2023	1.4	9.3	2010-2039	2.0	9.8	3.4	13.8
CMCC-CMS_rcp45_r1i1p1	2020-2049	2.3	2.5	2038-2067	3.1	-2.7	4.0	-3.5
CSIRO-Mk3-6-0_rcp45_r4i1p1	2021-2050	2.0	2.7	2038-2067	2.8	4.6	3.7	11.2
inmcm4_rcp45_r1i1p1	2047-2076	2.1	6.0	2071-2100 ¹	2.5	2.3	2.5	2.2
bcc-csm1-1_rcp85_r1i1p1	2006-2035	1.9	12.4	2023-2052	2.5	7.9	5.3	27.4
CanESM2_rcp85_r3i1p1	1999-2028	2.1	3.2	2012-2041	2.6	3.9	6.7	26.6
CMCC-CMS_rcp85_r1i1p1	2016-2045	2.6	-0.7	2027-2056	3.4	-4.1	6.8	-3.3
inmcm4_rcp85_r1i1p1	2029-2058	2.2	20.8	2044-2073	2.9	4.5	4.4	5.9

¹ The global 2.0 °C level is not reached within the 21st century. Therefore 2071-2100 is chosen as time slice

the average of 30-year time slices and comparing them to the average temperature during the pre-industrial period (1861–1890, PI). We start by comparing 1891–1920 to PI and iteratively move the 30-year time slice 1 year forward in time to identify for each GCM the earliest time slices where the global temperature increase thresholds of 1.5 and 2.0 °C compared to PI levels are reached (Table 1). For those time slices, we analyze for each GCM run how the regional temperature and precipitation have changed for the IGB basins with respect to the PI period, to identify how the regional temperature changes correspond to global temperature change (Table 1). Furthermore, we analyze for each GCM run how regional temperature levels for the IGB basins will change between the end of the twenty-first century (EOC, 2071–2100) and the PI era. Besides changes in mean air temperature, we analyze regional precipitation changes for the mentioned time slices, for each GCM run (Table 1).

Analysis of future changes in climate change indicators for 1.5 and 2.0 °C global temperature increase scenarios

We analyze changes in a set of ten climate change indicators (Table 2) for the 1.5 °C time slice, 2.0 °C time slice, and end of century projections for RCP4.5 and RCP8.5, compared to the reference period (REF, 1981–2010). These analyses are done by comparing the downscaled bias-corrected future GCM data to the reference climate dataset. In contrast to the analyses described in the “Extraction and analysis of GCM time slices of 1.5 and 2.0 °C global temperature increase with respect to the preindustrial era” section, here, we compare the future to the reference period, and not to the pre-industrial period, to focus on changes that are yet to come, and not on changes that have already happened between the pre-industrial period and the reference period. The eight GCMs’ time slices for the 1.5 °C

scenario are averaged to get an ensemble mean and the same is done for the time slices for the 2.0 °C. For the end of century projections for RCP4.5 and RCP8.5, respectively, the four members of each RCP are averaged for 2071–2100 to get their ensemble means.

The indicators have been selected in such a way that they can be directly or indirectly linked to the most important climate change impacts in the region, as identified in this study and by others (Kilroy 2015; Vinke et al. 2017) (Table 2), and can be derived from daily precipitation and daily mean, and maximum and minimum air temperature.

In this study, monsoon precipitation is defined as the precipitation falling during the months of June to September. The variability of precipitation is calculated as the coefficient of variation (CV), being the ratio of the standard deviation to the mean. To calculate the inter-annual variability, the mean and standard deviation are calculated from annual precipitation sums within a 30-year time slice. To calculate the intra-annual variability, the CV is calculated for each year within a 30-year time slice using the mean and standard deviation of daily precipitation sums within that year. Subsequently, the 30 CV values are averaged. To calculate the maximum 5-day precipitation sum, the maximum sum of precipitation falling during five consecutive days within a climatological period of 30 years (i.e., a full 30-year time slice) is calculated. The reference evapotranspiration is calculated using the Modified Hargreaves equation, which requires daily maximum, minimum, and mean air temperature as input (Droogers and Allen 2002). The obtained values are averaged over the years within a 30-year period. Consecutive dry days periods are calculated for a climatological period of 30 years as the number of consecutive days with precipitation $< 1 \text{ mm day}^{-1}$. Hot nights are defined as days with minimum air temperature $> 21 \text{ °C}$. The number of hot nights within each individual year is calculated, and the annual values are averaged for a 30-year period.

Table 2 Climate change indicators and the sectors affected by changes therein

Indicator	Symbol (unit)	Impact
Mean air temperature	T_{AVG} (°C)	Cryosphere degradation, disease transmissivity
Annual precipitation	P_{ANNUAL} (mm yr ⁻¹)	Agricultural production, hydropower production
Monsoon (June–September) precipitation	P_{MONSOON} (mm yr ⁻¹)	Agricultural production, floods, hydropower production
Precipitation inter-annual variability (Coefficient of Variation)	$P_{\text{CV-INTER ANNUAL}}$ (-)	Drought, Agricultural production, floods, hydropower production, environmental flows
Precipitation intra-annual variability (Coefficient of Variation)	$P_{\text{CV-INTRA-ANNUAL}}$ (-)	Drought, Agricultural production, floods, hydropower production, environmental flows
99 th percentile of daily precipitation sums	P_{99} (mm d ⁻¹)	Floods, landslides, debris flows, GLOFs, hydropower production
Maximum 5-day precipitation	$P_{5\text{DAY}}$ (mm)	Floods, landslides, debris flows, GLOFs, hydropower production
Reference evapotranspiration	ET_{REF} (mm yr ⁻¹)	Agricultural production
Consecutive dry days	CDD (n)	Drought, Agricultural production, hydropower production, environmental flows
Hot nights per year	HN (n yr ⁻¹)	Heat, human health

Results

Validation of GCM downscaling and bias-correction

Figure 2 shows that for both precipitation and air temperature the biases of the uncorrected GCM data are drastically reduced by the quantile mapping approach and the downscaled data matches well with the observed dataset. For daily mean air temperature values, the remaining biases are very close to zero for means and extremes. The same holds for daily maximum and minimum air temperatures (Supplementary Fig. S1). At the high ends of the distributions of precipitation values, in particular for the 99th percentile values of precipitation, some bias remains. This is most likely due to the generation of new extremes by extrapolating the quantile mapping error function linearly outside the range of the empirical cumulative distribution functions. However, the remaining biases are in the order of several percents and the largest bias is still below 10% (RCP 4.5 CSIRO-Mk3-6-0 r4i1p1 model in the Ganges basin). We therefore conclude that the

downscaled GCM data is suitable for our purpose to estimate future changes in climate change indicators.

Future climate change in the Indus, Ganges, and Brahmaputra river basins

The first striking result is the difference in warming of the IGB regional average compared to the global average. A global average warming of 1.5 °C with respect to PI levels would mean a warming of 1.4–2.6 ($\mu = 2.1$) °C for the IGB (Table 1). At 2.0 °C global average warming, the IGB would have warmed up by 2.0–3.4 ($\mu = 2.7$) °C. This difference can be largely attributed to elevation-dependent warming in the upstream IGB basins, i.e., the stronger warming of areas at high altitude compared to low-lying areas (Pepin et al. 2015; Palazzi et al. 2016). The South Asian river basins are therefore especially susceptible to climate change. Limiting global warming to 1.5 °C, or even 2.0 °C, proves to be very ambitious (Raftery et al. 2017), although not impossible (Rogelj

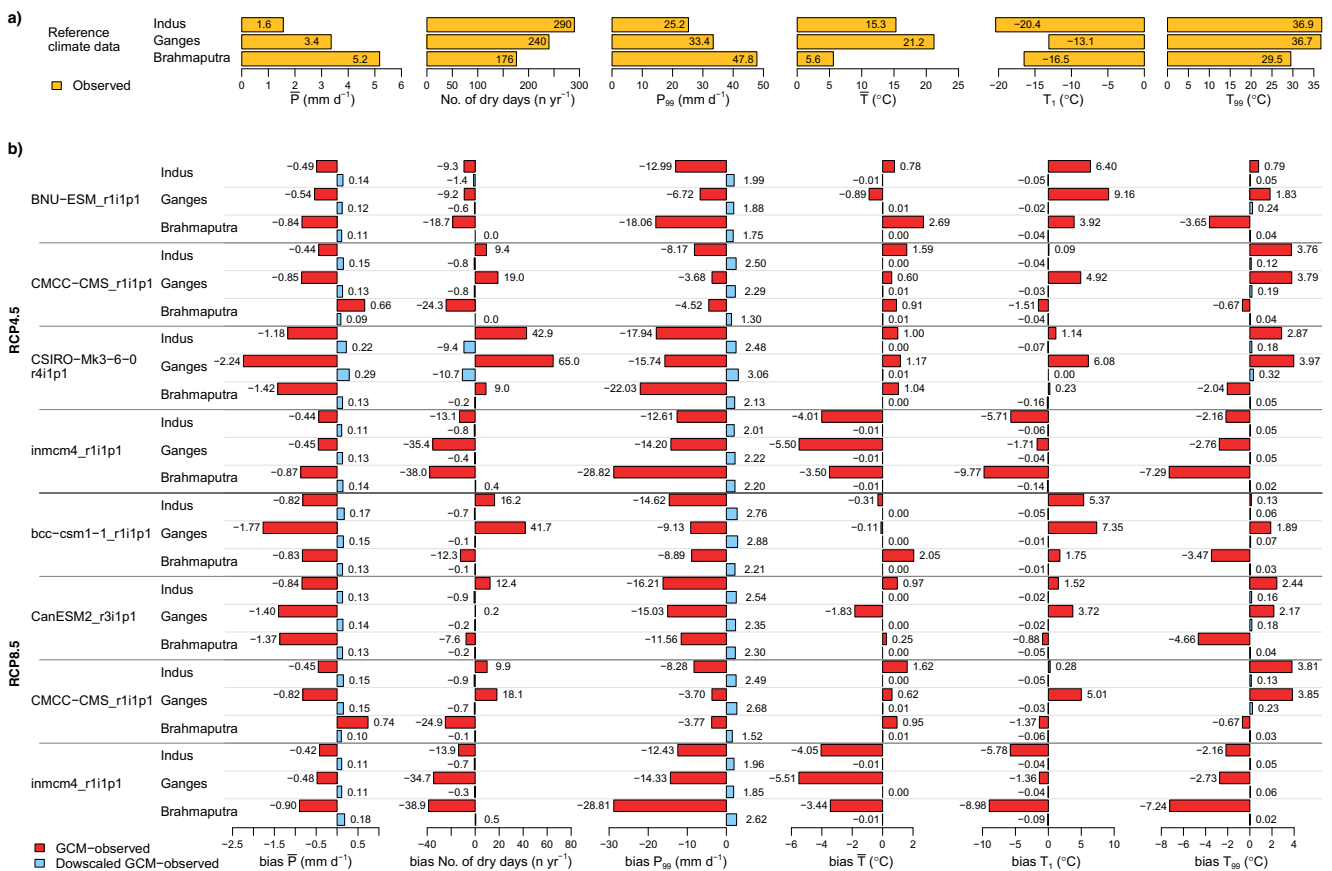


Fig. 2 Validation results for downscaled GCM runs. **a** Daily mean precipitation sum (\bar{P}), number of dry days per year, 99th percentile value of daily precipitation (P_{99}), mean of daily mean air temperature (\bar{T}), 1st percentile value of daily mean air temperature (T_1), 99th percentile values of daily mean air temperature (T_{99}) according to the reference climate dataset

for 100 randomly sampled grid cells in each river basin. **b** Biases of variables listed under (a) at the same 100 randomly sampled grid cells in each river basin in raw GCM data versus the reference climate dataset (GCM minus observed) and downscaled GCM data versus the reference climate dataset (downscaled GCM minus observed)

et al. 2016; Schleussner et al. 2016a; Millar et al. 2017). Our ensemble of representative scenarios for the IGB for RCP4.5 and RCP8.5, which may include more likely scenarios, indicates a regional temperature increase of 2.5–4.0 ($\mu = 3.4$) °C and 4.4–6.8 ($\mu = 5.8$) °C respectively by the end of the century, compared to PI levels.

For the 1.5 °C scenario, temperature in the IGB is increasing ≈ 1.15 °C with respect to the reference period (REF) (Fig. 3), meaning that temperature has already risen by ≈ 0.95 °C between REF and PI. For the 2.0 °C scenario, temperature increase in the IGB is ≈ 1.5 °C with respect to REF. Temperature increases differ spatially, and are strongest in the lower Indus basin and on the Tibetan Plateau. Precipitation most likely increases for the entire IGB, with strongest relative increases in the most southern part of the Indus basin and southwestern part of the Ganges basin (Fig. 3). The southern part of the Indus basin is very arid (Fig. 1b), and thus even large relative increases do not result in large amounts of precipitation in the future. Furthermore, the range in the precipitation projections is large, especially for the areas where the mean of the projections indicates large precipitation increases.

For monsoon precipitation, the spatial patterns are similar to the changes in average annual totals of precipitation (Fig. 4a–c). Striking is the small decrease in monsoon precipitation in the eastern part of the Brahmaputra basin for the 1.5 °C scenario. The intra-annual variability in precipitation decreases in the mountains, which may indicate increasing winter precipitation from westerly flows (Fig. 4d–f). For most of the lower basins, an increase in intra-annual variability is projected, which can be linked to the projected increases in monsoon precipitation. The inter-annual variability of precipitation likely decreases in areas with low inter-annual variability and increases in areas with already high inter-annual variability (Fig. 4g–i).

Extreme precipitation (Fig. 4j–o) shows a very clear trend with increases for most of the IGB domain. Only the west of the Indus basin shows decreases in P_{99} , which are stronger for the 1.5 °C scenario than the 2.0 °C scenario. The largest increases are projected for the Ganges basin (Table 3) and the very upstream parts of the Indus basin. Largest increases in 5-day sums of precipitation are projected for the Himalayan mountain range in the upper Indus basin. For the remaining areas, 5-day sums increase in general by 50–100%, with a few

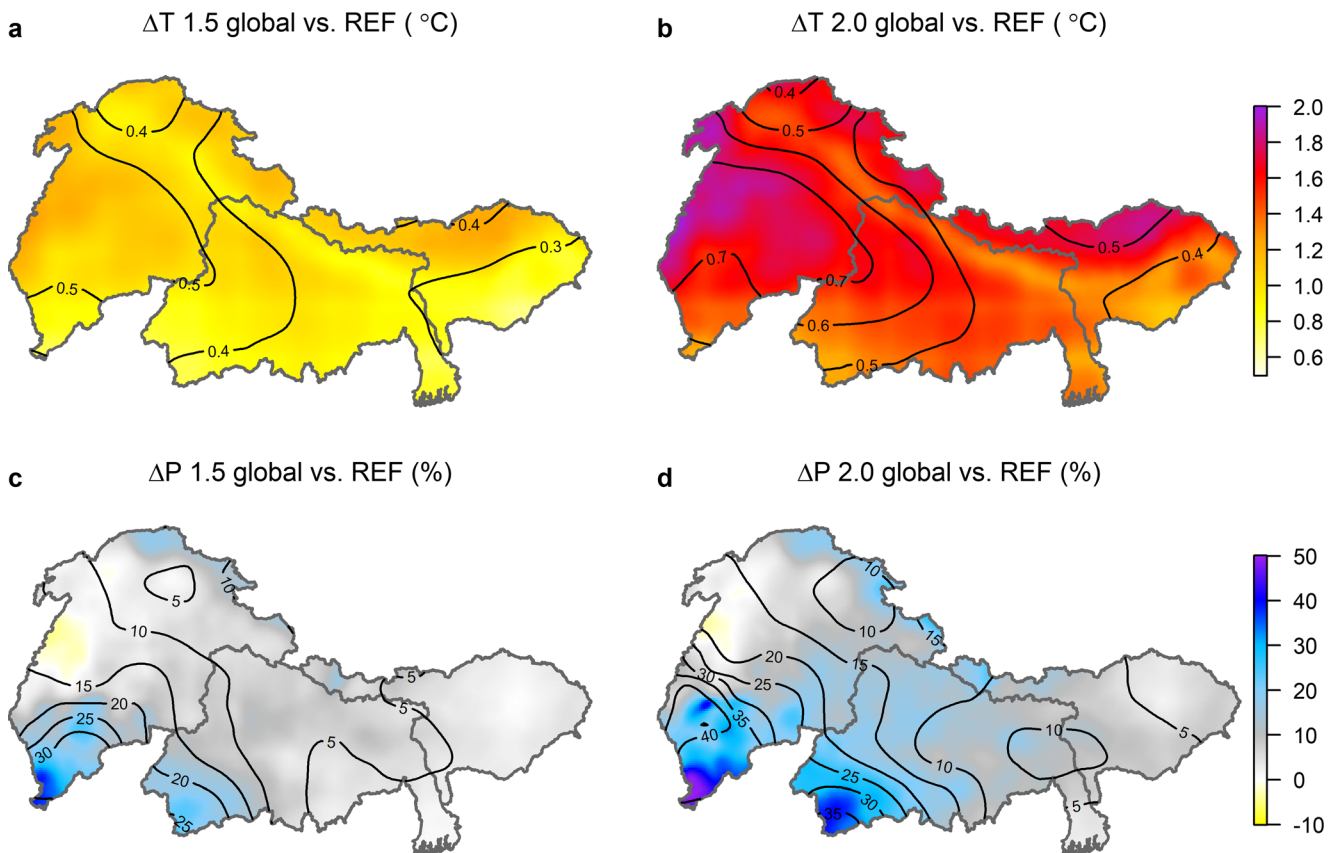


Fig. 3 Projected changes in mean annual air temperature (a, b) and mean annual precipitation (c, d) for the 1.5 °C and 2.0 °C scenarios with respect to the reference period (REF, 1981–2010). Grid values indicate the ensemble mean value and contour lines the ensemble ranges

exceptions of decreases in 5-day sums. Reference evapotranspiration increases for most of the IGB domain as a result of increasing temperatures (Fig. 4p–r). The increases are mostly around $+0.1 \text{ mm day}^{-1}$, which does not make a large difference for the plains where reference evapotranspiration is in the order of $3\text{--}4 \text{ mm day}^{-1}$, but is substantial for the mountainous upstream basins where reference evapotranspiration is in the order of 1 mm day^{-1} . Stronger absolute increases are projected for the Ganges-Brahmaputra delta and western Indus basin, whereas a decrease in reference evapotranspiration is projected for the Indus delta.

Interesting is that the length of dry periods decreases for the southern Indus basin, which is currently very prone to droughts (Fig. 4s–u). The length of dry periods also decreases in the Karakoram mountain range, which may be related to increases in winter precipitation. In the Brahmaputra basin, a decrease in dry periods' length is projected, but for the Ganges basin, the length of dry periods increases (Table 3). These contrasting trends may be related to the contrasting trends in intra-annual variability of precipitation in those two basins (Fig. 4d–f).

The number of hot nights increases for all areas, except for the areas at high altitude, where the threshold for hot nights is not reached. The most drastic increases are in areas in the foothills of the mountains, where the threshold was not reached in the reference period, but will be reached in the future (Fig. 4v–x). We analyzed the changes in the number of hot nights specifically for five major cities in the region, with large, growing, populations, located in different parts of the region (Fig. 5). Remarkable is the observation that the difference between the 1.5 and 2.0 °C scenarios is rather small. Increases are particularly drastic for the RCP8.5 EOC scenario. For relatively cool cities like Kathmandu, the occurrence of hot nights in the future will be a new phenomenon. For cities already facing severe heat stress, like Karachi, the number of hot nights per year can increase to up to 300 nights per year (Fig. 5d). Urban heat island effects have not been taken into account in our analysis, meaning that the found numbers may be underestimates.

Figure 6 shows the difference between the precipitation and ET_{REF} for both the kharif (monsoon) and rabi (winter) seasons. This is shown for two irrigated command areas located in the Indus and Ganges basins (Fig. 1a). The relation between P and ET_{REF} is an indicator of water availability for the crops in the irrigated command area. The change in precipitation for the command area in the Indus basin is small and the climate effect on ET_{REF} is small, $P-ET_{REF}$ is not expected to change much. The deficit likely increases slightly for the rabi season and decreases slightly for the kharif season, with roughly the same magnitude for each of the

four scenarios. For the command area in the Ganges basin, water availability is likely to increase in the kharif season and this is mostly a result of a strong climate signal in the precipitation. The projected precipitation increases for the RCP4.5 and RCP8.5 EOC projections are significantly stronger than for the 1.5 and 2.0 °C scenarios (Table 3), resulting in stronger increases in $P-ET_{REF}$. For the rabi season, the changes in the Ganges basin are similar to changes in the Indus basin. For both command areas, the uncertainty is much higher during the kharif season compared to the rabi season. This is because precipitation amounts are much higher during the kharif season compared to the rabi season, and therefore also the uncertainty in the precipitation amounts.

Discussion

Impacts of changes

From the results, it is clear that significant changes in the region are imminent for each of the scenarios. The likely increases in monsoon precipitation and precipitation extremes could possibly lead to more frequent and more severe flooding in the region in the future. The changes in precipitation sums and extremes both show a reasonable linear correlation with temperature increase (Fig. 7b–g). Strongest increases are projected for the Ganges basin, indicating that future flooding could be a major issue in this basin, even for the 1.5 °C scenario, while flooding is a major issue already in the present situation (e.g., the large floods during the 2017 monsoon season). A study comparing the impacts of 1.5 and 2.0 °C global temperature increase for water availability and hydrological extremes in the Brahmaputra river concludes indeed that flooding events will be more frequent and more severe at 2.0 °C global warming compared to 1.5 °C (Mohammed et al. 2017). The increases in frequency and magnitude of precipitation extremes, and possible associated increases in floods, sedimentation, landslides, and GLOFs negatively affect human lives and livelihoods and ecosystems. Also, adverse effects on infrastructure can possibly be expected, including hydropower infrastructure, which is rapidly developing in the region (Siddiqi et al. 2012; Molden et al. 2014).

The overall likely increase in annual precipitation totals could imply overall increases in water availability. However, because interannual and intra-annual variability in precipitation in general increase for the Indus and Ganges basins, the increase in water availability could possibly be not directly beneficial. In the Ganges basin, there could possibly be more periods of water excess and more periods of water shortage, as indicated by the increase in extreme precipitation and increase in dry periods (Fig. 7f–h). Although the dry periods show an overall decrease in the Indus and Brahmaputra basin (Fig. 7h),

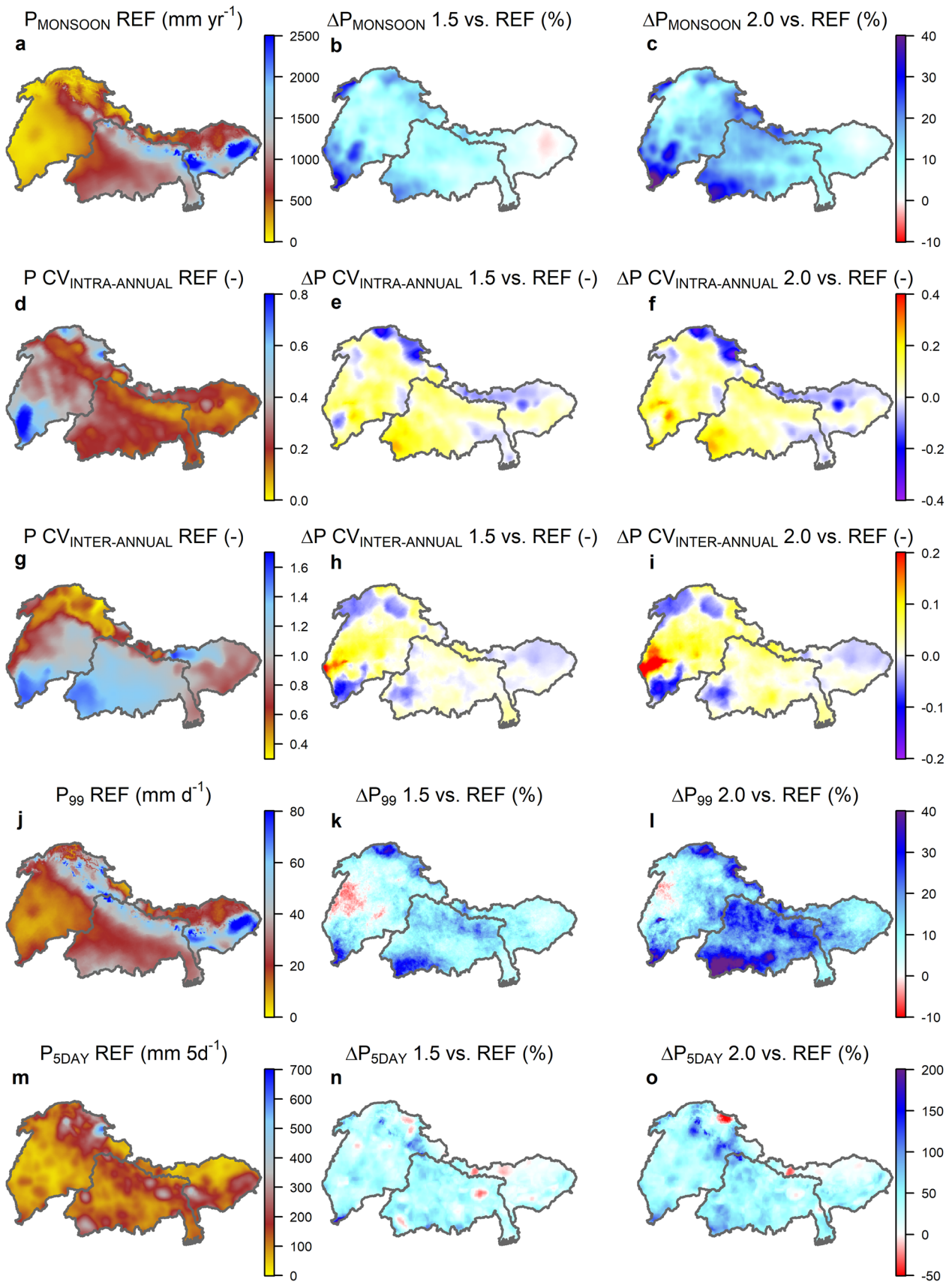


Fig. 4 Values of climate change indicators for the reference period (REF, 1981–2010, left column), and projected changes for the 1.5 °C scenario (middle column) and 2.0 °C scenario (right column) with respect to REF. The maps for the scenarios show the ensemble mean value

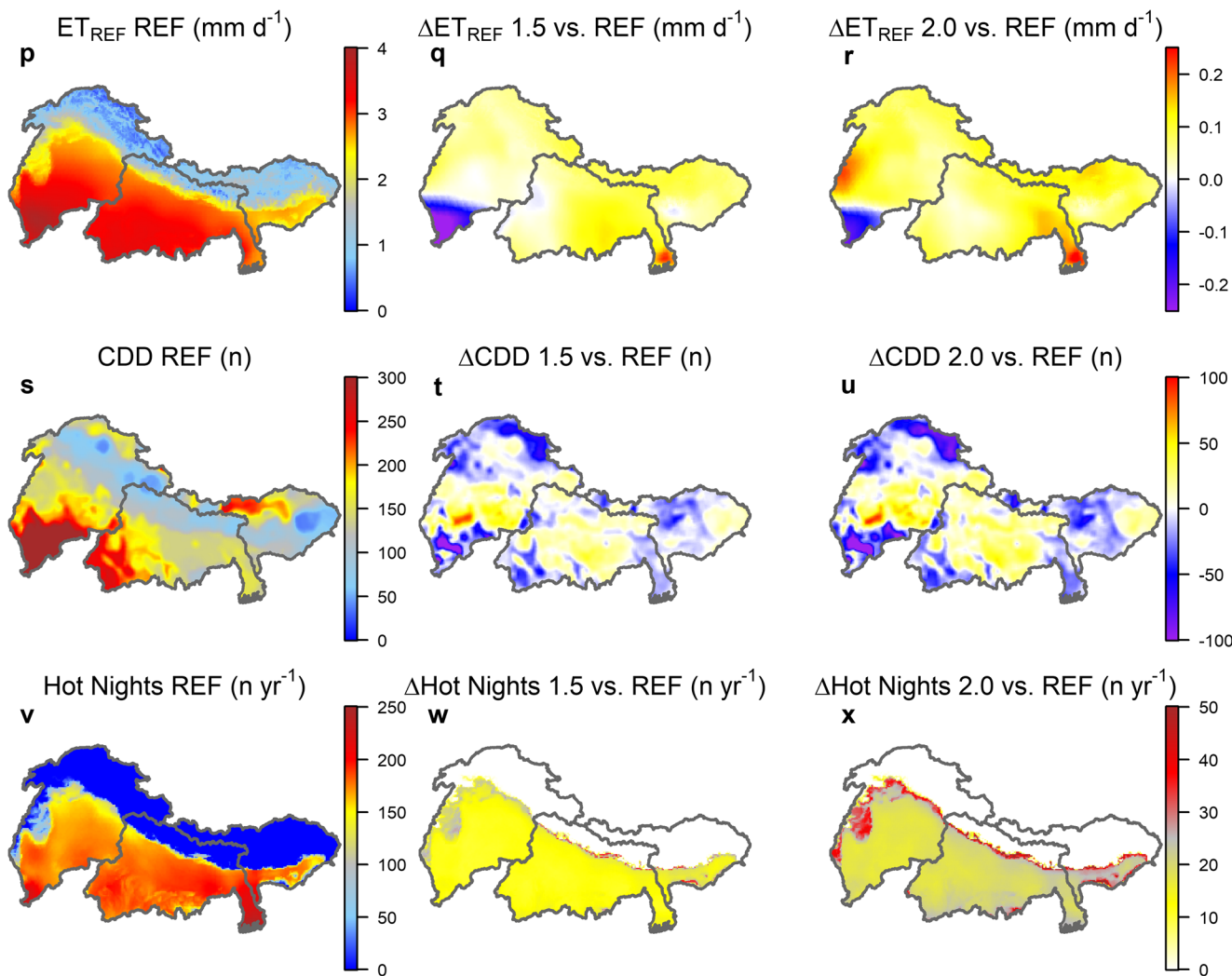


Fig. 4 (continued)

this is partly misleading because in the Indus the decrease in dry periods is mainly observed in the upstream mountainous parts of the basin (Fig. 4t, u), where drought is less of an issue compared to the downstream areas, where most of the agricultural areas and people are located. Nevertheless, the length of dry periods in the downstream areas shows only minor increases for the 1.5 and 2.0 °C scenarios, in line with results from a global study on changes in drought risk at 1.5 and 2.0 °C scenarios (Lehner et al. 2017). Despite minor changes in the number of dry periods, the likely increases in reference evapotranspiration indicate increasing crop water demands, which could put further stress on water resources.

As the Indus, Ganges, and Brahmaputra rely to varying extent on water supplied by upstream melt water, future changes in snow and ice have to be considered here as well. With likely increases in dry periods and more erratic precipitation, water supplied by snow and glacier melt may become more important in the future. Kraaijenbrink et al. (2017) show that the ice volume in Asia will decrease by \approx

36% under the 1.5 °C scenario and \approx 51–64% under RCP4.5 and RCP8.5 respectively. In particular, in the Indus basin, with high dependency on melt water (Lutz et al. 2014), this will affect future water availability. Further increases in the number of hot nights could affect human health further in a region where heat stress is already a major problem. Densely populated areas which have not encountered severe heat until now will likely also face this issue in the future, under each of the scenarios.

Concerning differences in impacts at 1.5 and 2.0 °C global temperature increase, we can draw the general conclusion that changes in climate change indicators other than air temperature correlate linearly with temperature increase (Fig. 7). For some indicators, we even observe a somewhat flattening trend with temperature increase (Fig. 7d–j). This is especially pronounced for the change in interannual variability of precipitation, which shows little difference between the 1.5 and 2.0 °C scenarios (Fig. 7d). In this case, for the Brahmaputra basin, the change becomes even negative for the 2.0 °C scenario. As the change in interannual variability in this study depends on change in the

Table 3 Basin-averaged values climate change indicators for the reference period (1981-2010, REF) and projected values of climate change indicators for the 1.5 °C, 2.0 °C and RCP4.5 and RCP8.5 end

of century (2071-2100, EOC) scenarios. Values indicate the ensemble mean value. Values in parentheses indicate the ensemble ranges

Indicator	River Basin	REF	1.5 °C	2.0 °C	EOC RCP4.5	EOC RCP8.5
T _{AVG} [°C]	Indus	14.8	15.9 (15.2 – 16.6)	16.5 (15.7 – 17.4)	17.3 (16 – 18.4)	19.1 (17.5 – 20.4)
	Ganges	21.4	22.4 (21.8 – 22.9)	22.9 (22.3 – 23.7)	23.6 (22.6 – 24.6)	25.1 (24.0 – 26.3)
	Brahmaputra	6.0	7 (6.5 – 7.3)	7.5 (6.9 – 8.1)	8.1 (7.2 – 8.9)	9.7 (8.6 – 10.7)
P _{ANNUAL} [mm yr ⁻¹]	Indus	616	662 (603 – 762)	695 (571 – 810)	705 (612 – 812)	693 (567 – 787)
	Ganges	1245	1346 (1248 – 1549)	1443 (1248 – 1736)	1501 (1287 – 1611)	1549 (1212 – 1753)
	Brahmaputra	1861	1931 (1883 – 2009)	2009 (1891 – 2131)	2041 (1931 – 2143)	2418 (2096 – 2861)
P _{MONSOON} [mm yr ⁻¹]	Indus	301	335 (283 – 395)	348 (286 – 409)	370 (339 – 403)	363 (274 – 441)
	Ganges	1016	1098 (1038 – 1266)	1175 (1048 – 1445)	1239 (1090 – 1341)	1274 (1002 – 1507)
	Brahmaputra	1307	1342 (1305 – 1406)	1401 (1315 – 1511)	1419 (1336 – 1520)	1717 (1465 – 2071)
P _{CV-INTER-ANNUAL} [-]	Indus	0.37	0.41 (0.38 – 0.48)	0.42 (0.34 – 0.49)	0.45 (0.37 – 0.63)	0.46 (0.44 – 0.49)
	Ganges	0.20	0.27 (0.21 – 0.37)	0.27 (0.20 – 0.35)	0.27 (0.19 – 0.35)	0.3 (0.28 – 0.34)
	Brahmaputra	0.17	0.17 (0.13 – 0.23)	0.16 (0.14 – 0.17)	0.16 (0.14 – 0.17)	0.17 (0.17 – 0.18)
P _{CV-INTRA-ANNUAL} [-]	Indus	0.86	0.87 (0.81 – 0.98)	0.89 (0.74 – 0.99)	0.93 (0.79 – 0.98)	0.82 (0.62 – 0.95)
	Ganges	1.19	1.19 (1.14 – 1.26)	1.2 (1.09 – 1.28)	1.24 (1.18 – 1.28)	1.2 (1.11 – 1.31)
	Brahmaputra	0.95	0.94 (0.92 – 0.98)	0.95 (0.91 – 0.98)	0.96 (0.91 – 1.01)	0.98 (0.95 – 1.02)
P ₉₉ [mm d ⁻¹]	Indus	22.8	24.5 (22.7 – 26.8)	25.6 (22.1 – 28.9)	27.6 (25.3 – 31.5)	27.3 (23.8 – 31.4)
	Ganges	32.0	36 (32.9 – 42.8)	39.5 (33.5 – 50.1)	43.7 (35.7 – 48.3)	46.7 (36.2 – 54.9)
	Brahmaputra	40.4	43.4 (42.3 – 44.8)	46.1 (43.8 – 48.1)	48.1 (45.7 – 50.1)	64.2 (54.1 – 83.8)
P _{SDAY} [mm]	Indus	118	153 (168 – 139)	163 (217 – 139)	179 (241 – 146)	189 (237 – 159)
	Ganges	142	179 (227 – 144)	189 (215 – 159)	207 (275 – 177)	234 (282 – 174)
	Brahmaputra	130	145 (178 – 130)	154 (176 – 131)	161 (179 – 144)	193 (233 – 164)
CDD [n]	Indus	172	167 (188 – 142)	162 (190 – 143)	161 (189 – 144)	127 (211 – 2)
	Ganges	152	154 (176 – 130)	157 (175 – 130)	161 (185 – 147)	118 (186 – 3)
	Brahmaputra	121	115 (125 – 106)	112 (123 – 93)	113 (118 – 106)	86 (122 – 3)
ET _{REF} [mm d ⁻¹]	Indus	2.26	2.27 (2.37 – 2.16)	2.32 (2.44 – 2.17)	2.41 (2.54 – 2.34)	2.46 (2.55 – 2.38)
	Ganges	2.79	2.86 (2.97 – 2.72)	2.87 (3.07 – 2.65)	2.85 (3.07 – 2.51)	2.99 (3.16 – 2.8)
	Brahmaputra	1.54	1.6 (1.66 – 1.54)	1.63 (1.69 – 1.59)	1.89 (2.42 – 1.67)	1.74 (1.83 – 1.69)
HN [n yr ⁻¹]	Indus	95	104 (110 – 98)	108 (116 – 102)	113 (121 – 102)	131 (143 – 113)
	Ganges	147	158 (164 – 152)	165 (172 – 159)	173 (182 – 159)	192 (208 – 171)
	Brahmaputra	39	44 (47 – 41)	47 (51 – 44)	51 (56 – 44)	59 (66 – 49)

mean (and therefore total) and standard deviation of precipitation, this may be related to the strong increases in monsoon

precipitation (Table 3, Figs. 4 b, c and 7c). Striking are also the earlier mentioned opposing trends in changes in the length

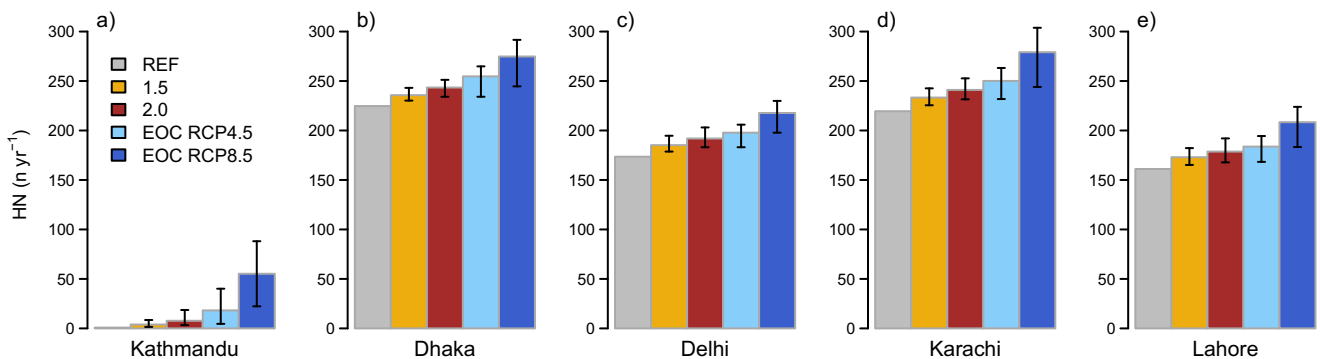


Fig. 5 Hot nights per year under different scenarios in major cities in the study region. Bars indicate the ensemble mean. Error bars indicate the ensemble range. Locations of the cities are indicated in Fig. 1

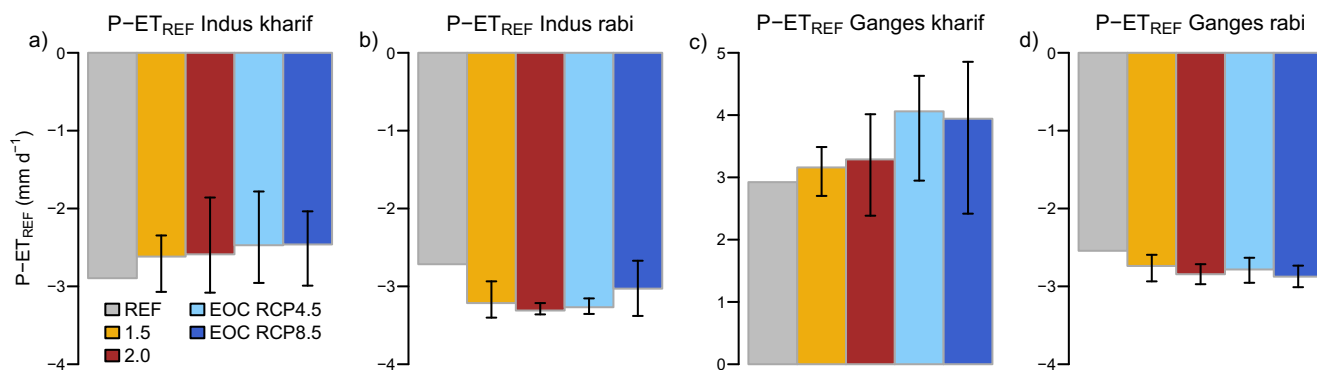


Fig. 6 Future precipitation minus evapotranspiration for irrigated command areas in the Indus (a) and Ganges basin (b), for the kharif and rabi seasons. Plotted values indicate the ensemble means. The command areas are indicated in Fig. 1

of dry periods between the Indus and Brahmaputra on one hand and the Ganges on the other (Fig. 7h). On the whole, we can conclude that the regional impacts of climate change will be more severe for the 2.0 °C than the 1.5 °C scenario.

Much more important however are the large differences in changes between the 1.5 °C and 2.0 °C scenarios on the one hand, and the more likely RCP4.5 and RCP8.5 scenarios on the other hand. As regional temperature increases under the RCP4.5 and RCP8.5 end of century scenarios are significantly higher than for the 1.5 °C and 2.0 °C scenarios (Table 1), the changes in other climate change indicators, and their impacts in different sectors are also much stronger (Table 3). Current global warming is already close to 1 °C with respect to pre-industrial temperature levels. Even considering the effects of emission mitigation policies, the chances that global temperature

increase will be kept below 2.0 °C are small. We therefore stress that the 1.5 °C (or even the 2.0 °C) scenario is not suitable for climate change adaptation planning, and it is therefore undesirable that the 1.5 °C scenario will become a new paradigm. We emphasize that the formulation of robust climate change adaptation policies should be based on the full range of climate change projections.

Uncertainties and limitations

By using an ensemble of GCMs, we include the uncertainty in future climate in our assessment. This uncertainty is rather large, as illustrated in Figs. 3 and 5, and Tables 1 and 3. The changes in climate change indicators associated with a 1.5 or 2.0 °C global temperature increase have wide ranges. This implies that care must be taken in interpreting the results. In our

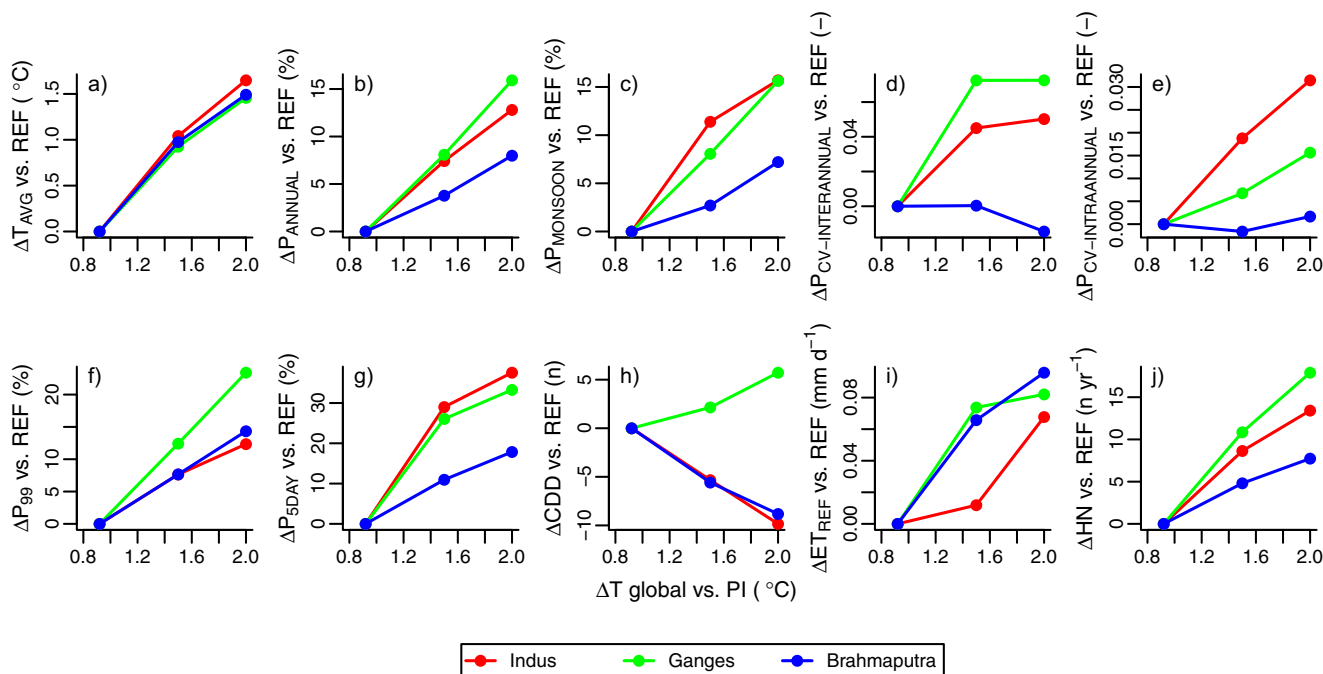


Fig. 7 Basin-averaged changes in climate change for the 1.5 °C and 2 °C scenarios with respect to the reference period (1981–2010, REF, ΔT global vs. PI = 0.92). Plotted values indicate the ensemble means

analysis, we mostly discuss changes based on the ensemble mean, and it has to be taken into account that there are large uncertainty ranges associated with the ensemble mean values. The uncertainty in future climate can be largely attributed to the general poor skill of GCMs in simulating the important regional climatological features of this region (Sperber et al. 2013; Palazzi et al. 2014; Ramesh and Goswami 2014; Sperber and Annamalai 2014; Mishra 2015). We reduced the uncertainty by only selecting GCMs with sufficient skill in simulating historical climate for the IGB region, but still large discrepancies in GCMs' ability to simulate the important features of the regional climate are evident (Lutz et al. 2016b).

Our ensemble of GCMs has been selected based on the range in the projections over the entire IGB. This scale issue may mean that the full range of projections is not captured for each separate area within the IGB. Because of the regional scale of the study, we analyze climate data at 10×10 -km spatial resolution. Climatic processes at smaller scales, which in many cases dictate the actual impact, may be insufficiently represented.

Our study forms a first-order quantitative assessment of the difference in regional impacts of climate change at 1.5 and 2.0 °C global temperature increase scenarios. We link quantitative changes in a set of ten climate change indicators to expected impacts for different sectors. Although we show that the changes in the analyzed climate change indicators increase in general linear with air temperature, on the impact side many processes may respond in a non-linear fashion to changes in climate change indicators. To quantify and verify the suggested impacts and differences in impacts of these scenarios for the different sectors requires additional sector-specific modeling studies in the fields of, i.e., hydrology, food and energy production, disease transmission, and natural hazards. It also requires inclusion of the projected future socio-economic changes in the region. With an expected strong continued population growth, pressure on natural resources in the region will increase, as well as the number of people who are prone to climate change induced natural disasters. Our analysis of ten climate change indicators based on air temperature and precipitation does not include future changes in sea level rise, although this is an important climate hazard in the Ganges-Brahmaputra delta. A recent study investigating the differences in impacts from sea level rise resulting from 1.5, 2.0, and 3.0 °C global temperature rise concludes for this delta that in unprotected areas the flooding depth is projected to double at 3.0 °C compared to 1.5 °C. In protected areas, this increase is approximately 50%. The average area inundated would increase 2.5 times (Brown et al. 2018).

Conclusions

South Asian river basins are vulnerable to climate change. A global temperature increase of 1.5 °C with respect to pre-

industrial levels would imply a ≈ 2.1 °C temperature increase for the Indus, Ganges, and Brahmaputra river basins. Under a 2.0 °C global temperature increase scenario, these river basins would warm up by ≈ 2.7 °C. Our analysis of changes in climate change indicators under these scenarios shows that the region could face strong negative impacts of climate change for the occurrence of floods, agricultural production, hydropower production, and human health. The changes in climate change indicators are in general linearly increasing with temperature increase.

However, more likely scenarios for RCP4.5 and RCP8.5 imply regional temperature increases of ≈ 3.4 and ≈ 5.8 °C at the end of the twenty-first century, and therefore possibly much stronger regional impacts. We stress that the 1.5 °C (or even the 2.0 °C) scenario is not suitable for robust climate change adaptation planning, and emphasize that the formulation of robust climate change adaptation policies should be based on the full range of climate change projections.

Acknowledgements We acknowledge the World Climate Research Program's Working Group on Coupled Modeling, which is responsible for CMIP5, and we thank the climate modeling groups for producing and making available their model output. We thank an anonymous reviewer and editor Erika Coppola for constructive comments which significantly improved the manuscript. We are grateful to Evans Kituyi for facilitating the CARIIA cross-consortia work on 1.5 degrees.

Disclaimer The views and interpretations in this publication are those of the authors and are not necessarily attributable to their affiliated organizations.

Funding information This work was carried out by the Himalayan Adaptation, Water and Resilience (HI-AWARE) consortium under the Collaborative Adaptation Research Initiative in Africa and Asia (CARIIA) with financial support from the United Kingdom's Department for International Development (DFID) and the International Development Research Centre (IDRC), Ottawa, Canada. The work is funded by IDRC's Opportunities and Synergies Fund as part of a CARIIA-wide cross-consortia activity on 1.5 degrees. The views expressed in this work are those of the creators and do not necessarily represent those of the UK Government's Department for International Development, the International Development Research Centre, Canada or its Board of Governors, and are not necessarily attributable to their organizations.

The study was partially supported by ICIMOD core funds (contributed by the Governments of Afghanistan, Australia, Austria, Bangladesh, Bhutan, China, India, Myanmar, Nepal, Norway, Pakistan, Switzerland and the United Kingdom).

The project has also received funding from the European Research Council (ERC) under the European Union's Horizon 2020 research and innovation program (grant agreement number 676819) and the Netherlands Organization for Scientific Research under the Innovational Research Incentives Scheme VIDI (grant agreement 016.181.308).

Compliance with ethical standards

Conflict of interest The authors declare that they have no conflict of interest.

Open Access This article is distributed under the terms of the Creative Commons Attribution 4.0 International License (<http://creativecommons.org/licenses/by/4.0/>), which permits unrestricted use, distribution, and reproduction in any medium, provided you give appropriate credit to the original author(s) and the source, provide a link to the Creative Commons license, and indicate if changes were made.

Publisher's Note Springer Nature remains neutral with regard to jurisdictional claims in published maps and institutional affiliations.

References

- Balaguru K, Taraphdar S, Leung LR, Foltz GR (2014) Increase in the intensity of postmonsoon Bay of Bengal tropical cyclones. *Geophys Res Lett* 41:3594–3601. <https://doi.org/10.1002/2014GL060197>
- Biemans H, Speelman LH, Ludwig F, Moors EJ, Wiltshire AJ, Kumar P, Gerten D, Kabat P (2013) Future water resources for food production in five South Asian river basins and potential for adaptation - a modeling study. *Sci Total Environ* 468–469:S117–S131. <https://doi.org/10.1016/j.scitotenv.2013.05.092>
- Bolch T, Kulkarni A, Kääb A, Huggel C, Paul F, Cogley JG, Frey H, Kargel JS, Fujita K, Scheel M, Bajracharya S, Stoffel M (2012) The state and fate of Himalayan glaciers. *Science* 336:310–314. <https://doi.org/10.1126/science.1215828>
- Brown S, Nicholls RJ, Lázár AN, Hornby DD, Hill C, Hazra S, Addo KA, Haque A, Caesar J, Tompkins E (2018) What are the implications of sea-level rise for a 1.5°C, 2°C and 3°C rise in global mean temperatures in vulnerable deltas? *Reg Environ Chang* 18:1829–1842. <https://doi.org/10.1007/s10113-018-1311-0>
- Brun F, Berthier E, Wagnon P, Kääb A, Treichler D (2017) A spatially resolved estimate of High Mountain Asia glacier mass balances, 2000–2016. *Nat Geosci* 10:668–673. <https://doi.org/10.1038/ngeo2999>
- Clemençon R (2016) The two sides of the Paris climate agreement: dismal failure or historic breakthrough? *J Environ Dev* 25:3–24. <https://doi.org/10.1177/10704965166631362>
- De Souza K, Kituyi E, Harvey B, Leone M, Murali KS, Ford JD (2015) Vulnerability to climate change in three hot spots in Africa and Asia: key issues for policy-relevant adaptation and resilience-building research. *Reg Environ Chang* 15:747–753. <https://doi.org/10.1007/s10113-015-0755-8>
- Dhiman RC, Chavan L, Pant M, Pahwa S (2011) National and regional impacts of climate change on malaria by 2030. *Curr Sci* 101:372–383
- Droogers P, Allen RG (2002) Estimating reference evapotranspiration under inaccurate data conditions. *Irrig Drain Syst* 16:33–45. <https://doi.org/10.1023/A:1015508322413>
- Galewsky J (2009) Rain shadow development during the growth of mountain ranges: an atmospheric dynamics perspective. *J Geophys Res* 114:F01018. <https://doi.org/10.1029/2008JF001085>
- Gleeson T, Wada Y (2013) Assessing regional groundwater stress for nations using multiple data sources with the groundwater footprint. *Environ Res Lett* 8:044010. <https://doi.org/10.1088/1748-9326/8/4/044010>
- Gleeson T, Wada Y, Bierkens MFP, van Beek LPH (2012) Water balance of global aquifers revealed by groundwater footprint. *Nature* 488:197–200. <https://doi.org/10.1038/nature11295>
- Higgins SA, Overeem I, Steckler MS, Syvitski JPM, Seeber L, Akhter SH (2014) InSAR measurements of compaction and subsidence in the Ganges-Brahmaputra Delta, Bangladesh. *J Geophys Res Earth Surf* 119:1768–1781. <https://doi.org/10.1002/2014JF003117>
- Hirabayashi Y, Mahendran R, Koirala S, Konoshima L, Yamazaki D, Watanabe S, Kim H, Kanae S (2013) Global flood risk under climate change. *Nat Clim Chang* 3:816–821. <https://doi.org/10.1038/nclimate1911>
- Im E-S, Pal JS, Eltahir EAB (2017) Deadly heat waves projected in the densely populated agricultural regions of South Asia. *Sci Adv* 3:1–8. <https://doi.org/10.1126/sciadv.1603322>
- Immerzeel WW, Van Beek LP, Bierkens MFP (2010) Climate change will affect the Asian water towers. *Science* 328:1382–1385. <https://doi.org/10.1126/science.1183188>
- Immerzeel WW, Pellicciotti F, Bierkens MFP (2013) Rising river flows throughout the twenty-first century in two Himalayan glacierized watersheds. *Nat Geosci* 6:742–745. <https://doi.org/10.1038/ngeo1896>
- IPCC (2014) Climate change 2014: synthesis report. Contribution of Working Groups I, II and III to the Fifth Assessment Report of the Intergovernmental Panel on Climate Change [Core Writing Team, Pachauri RK, Meyer LA (eds)]. IPCC, Geneva, Switzerland, p 151
- IPCC (2018) Global warming of 1.5°C. An IPCC special report on the impacts of global warming of 1.5°C above pre-industrial levels and related global greenhouse gas emission pathways, in the context of strengthening the global response to the threat of climate change, sustainable development, and efforts to eradicate poverty [Masson-Delmotte V, Zhai P, Pörtner HO, Roberts D, Skea J, Shukla PR, Pirani A, Moufouma-Okia W, Péan C, Pidcock R, Connors S, Matthews JBR, Chen Y, Zhou X, Gomis MI, Lonnoy E, Maycock T, Tignor M, Waterfield T (eds)]. In Press
- Kay S, Caesar J, Wolf J, Bricheno L, Nicholls RJ, Saiful Islam AKM, Haque A, Pardaens A, Lowe JA (2015) Modelling the increased frequency of extreme sea levels in the Ganges-Brahmaputra-Meghna delta due to sea level rise and other effects of climate change. *Environ Sci Process Impacts* 17:1311–1322. <https://doi.org/10.1039/c4em00683f>
- Kilroy G (2015) A review of the biophysical impacts of climate change in three hotspot regions in Africa and Asia. *Reg Environ Chang* 15:771–782. <https://doi.org/10.1007/s10113-014-0709-6>
- Kraaijenbrink PDA, Bierkens MFP, Lutz AF, Immerzeel WW (2017) Impact of a 1.5 °C global temperature rise on Asia's glaciers. *Nature* 549:257–260. <https://doi.org/10.1038/nature23878>
- Lehner F, Coats S, Stocker TF, Pendergrass AG, Sanderson BM, Raible CC, Smerdon JE (2017) Projected drought risk in 1.5°C and 2°C warmer climates. *Geophys Res Lett* 44:7419–7428. <https://doi.org/10.1002/2017GL074117>
- Lutz AF, Immerzeel WW (2015) HI-AWARE reference climate dataset for the Indus, Ganges and Brahmaputra River basins. FutureWater report 146. Wageningen, The Netherlands
- Lutz AF, Immerzeel WW, Shrestha AB, Bierkens MFP (2014) Consistent increase in High Asia's runoff due to increasing glacier melt and precipitation. *Nat Clim Chang* 4:587–592. <https://doi.org/10.1038/NCLIMATE2237>
- Lutz AF, Immerzeel WW, Kraaijenbrink PDA, Shrestha AB (2016a) Climate change impacts on the upper Indus hydrology: sources, shifts and extremes. *PLoS One* 11:e0165630. <https://doi.org/10.1371/journal.pone.0165630>
- Lutz AF, ter Maat HW, Biemans H, Shrestha AB, Wester P, Immerzeel WW (2016b) Selecting representative climate models for climate change impact studies: an advanced envelope-based selection approach. *Int J Climatol* 36:3988–4005. <https://doi.org/10.1002/joc.4608>
- Mertz O, Halsnæs ÆK, Olesen ÆJE (2009) Adaptation to climate change in developing countries. *Environ Manag* 43:743–752. <https://doi.org/10.1007/s00267-008-9259-3>
- Millar RJ, Fuglestedt JS, Friedlingstein P, Rogelj J, Grubb MJ, Matthews HD, Skeie RB, Forster PM, Frame DJ, Allen MR (2017) Emission budgets and pathways consistent with limiting warming to 1.5 °C. *Nat Geosci* 10:741–748. <https://doi.org/10.1038/ngeo3031>

- Mirza MMQ (2011) Climate change, flooding in South Asia and implications. *Reg Environ Chang* 11:95–107. <https://doi.org/10.1007/s10113-010-0184-7>
- Mishra V (2015) Climatic uncertainty in Himalayan Water Towers. *J Geophys Res Atmos* 120:2689–2705. <https://doi.org/10.1002/2014JD022650>
- Mohammed K, Islam AS, tarekul IG, Alfieri L, Bala SK, Khan MJU (2017) Extreme flows and water availability of the Brahmaputra River under 1.5 and 2 °C global warming scenarios. *Clim Chang* 145:159–175. <https://doi.org/10.1007/s10584-017-2073-2>
- Molden DJ, Vaidya RA, Shrestha AB, Rasul G, Shrestha MS (2014) Water infrastructure for the Hindu Kush Himalayas. *Int J Water Resour Dev* 30:60–77. <https://doi.org/10.1080/07900627.2013.859044>
- NCC (2016) Editorial: researching 1.5 °C. *Nat Clim Chang* 6:975–975. <https://doi.org/10.1038/nclimate3154>
- Nicholls RJ, Cazenave A (2010) Sea-level rise and its impact on coastal zones. *Science* 328:1517–1520. <https://doi.org/10.1126/science.1185782>
- Pal JS, Eltahir EAB (2015) Future temperature in southwest Asia projected to exceed a threshold for human adaptability. *Nat Clim Chang* 6:197–200. <https://doi.org/10.1038/nclimate2833>
- Palazzi E, von Hardenberg J, Terzago S, Provenzale A (2014) Precipitation in the Karakoram-Himalaya: a CMIP5 view. *Clim Dyn* 45:21–45. <https://doi.org/10.1007/s00382-014-2341-z>
- Palazzi E, Filippi L, von Hardenberg J (2016) Insights into elevation-dependent warming in the Tibetan Plateau-Himalayas from CMIP5 model simulations. *Clim Dyn* 48:1–18. <https://doi.org/10.1007/s00382-016-3316-z>
- Pepin N, Bradley RS, Diaz HF, Baraer M, Caceres EB, Forsythe N, Fowler H, Greenwood G, Hashmi MZ, Liu XD, Miller JR, Ning L, Ohmura A, Palazzi E, Rangwala I, Schöner W, Severskiy I, Shahgedanova M, Wang MB, Williamson SN, Yang DQ (2015) Elevation-dependent warming in mountain regions of the world. *Nat Clim Chang* 5:424–430. <https://doi.org/10.1038/nclimate2563>
- Piani C, Haerter JO, Coppola E (2010) Statistical bias correction for daily precipitation in regional climate models over Europe. *Theor Appl Climatol* 99:187–192. <https://doi.org/10.1007/s00704-009-0134-9>
- Raftery AE, Zimmer A, Frierson DMW, Startz R, Liu P (2017) Less than 2 °C warming by 2100 unlikely. *Nat Clim Chang* 7:637–641. <https://doi.org/10.1038/nclimate3352>
- Ramesh KV, Goswami P (2014) Assessing reliability of regional climate projections: the case of Indian monsoon. *Nat Sci Rep* 4:4071. <https://doi.org/10.1038/srep04071>
- Rogelj J, Luderer G, Pietzcker RC, Kriegler E, Schaeffer M, Krey V, Riahi K (2016) Energy system transformations for limiting end-of-century warming to below 1.5 °C. *Nat Clim Chang* 6:538–538. <https://doi.org/10.1038/nclimate2993>
- Savarese A (2016) The Paris agreement: a new beginning? *J Energy Nat Resour Law* 34:16–26. <https://doi.org/10.1080/02646811.2016.1133983>
- Schleussner C-F, Rogelj J, Schaeffer M, Lissner T, Licker R, Fischer EM, Knutti R, Levermann A, Frieler K, Hare W (2016a) Perspective: science and policy characteristics of the Paris Agreement temperature goal. *Nat Clim Chang* 6:827–835. <https://doi.org/10.1038/NCLIMATE3096>
- Schleussner CF, Lissner TK, Fischer EM, Wohland J, Perrette M, Golly A, Rogelj J, Childers K, Schewe J, Frieler K, Mengel M, Hare W, Schaeffer M (2016b) Differential climate impacts for policy-relevant limits to global warming: the case of 1.5 °C and 2 °C. *Earth Syst Dyn Discuss* 7:327–351. <https://doi.org/10.5194/esd-7-327-2016>
- Shrestha A, Agrawal N, Alfthan B, Bajracharya S, Maréchal J, van Oort B (2015) The Himalayan climate and water Atlas: impact of climate change on water resources in five of Asia's major river basins. ICIMOD, GRID-Arendal, CICERO
- Siddiqi A, Wescoat JL, Humair S, Afridi K (2012) An empirical analysis of the hydropower portfolio in Pakistan. *Energy Policy* 50:228–241. <https://doi.org/10.1016/j.enpol.2012.06.063>
- Singh D, Tsiang M, Rajaratnam B, Di NS (2014) Observed changes in extreme wet and dry spells during the South Asian summer monsoon season. *Nat Clim Chang* 4:456–461. <https://doi.org/10.1038/NCLIMATE2208>
- Sperber KR, Annamalai H (2014) The use of fractional accumulated precipitation for the evaluation of the annual cycle of monsoons. *Clim Dyn* 43:3219–3244. <https://doi.org/10.1007/s00382-014-2099-3>
- Sperber KR, Annamalai H, Kang IS, Kitoh A, Moise A, Turner A, Wang B, Zhou T (2013) The Asian summer monsoon: an intercomparison of CMIP5 vs. CMIP3 simulations of the late 20th century. *Clim Dyn* 41:2711–2744. <https://doi.org/10.1007/s00382-012-1607-6>
- Tambe S, Kharel G, Arrawatia ML, Kulkarni H, Mahamuni K, Ganeriwala AK (2012) Reviving dying springs: climate change adaptation experiments from the Sikkim Himalaya. *Mt Res Dev* 32:62–72. <https://doi.org/10.1659/MRD-JOURNAL-D-11-00079.1>
- Tariq S, Mahmood A, Rasul G (2014) Temperature and precipitation: GLOF triggering indicators in Gilgit-Baltistan, Pakistan. *Pak J Meteorol* 10:39–56
- Taylor KE, Stouffer RJ, Meehl GA (2012) An overview of CMIP5 and the experiment design. *Bull Am Meteorol Soc* 93:485–498. <https://doi.org/10.1175/BAMS-D-11-00094.1>
- Thiemeßl MJ, Gobiet A, Heinrich G (2011a) Empirical-statistical downscaling and error correction of regional climate models and its impact on the climate change signal. *Clim Chang* 112:449–468. <https://doi.org/10.1007/s10584-011-0224-4>
- Thiemeßl MJ, Gobiet A, Leuprecht A (2011b) Empirical-statistical downscaling and error correction of daily precipitation from regional climate models. *Int J Climatol* 31:1530–1544. <https://doi.org/10.1002/joc.2168>
- Trenberth KE, Dai A, van der Schrier G, Jones PD, Barichivich J, Briffa KR, Sheffield J (2013) Global warming and changes in drought. *Nat Clim Chang* 4:17–22. <https://doi.org/10.1038/nclimate2067>
- Turner AG, Annamalai H (2012) Climate change and the South Asian summer monsoon. *Nat Clim Chang* 2:587–595. <https://doi.org/10.1038/nclimate1495>
- UN (2015) World population prospects, 2015 revision. New York
- van Vuuren DP, Edmonds J, Kainuma M, Riahi K, Thomson A, Hibbard K, Hurtt GC, Kram T, Krey V, Lamarque J-F, Masui T, Meinshausen M, Nakicenovic N, Smith SJ, Rose SK (2011) The representative concentration pathways: an overview. *Clim Chang* 109:5–31. <https://doi.org/10.1007/s10584-011-0148-z>
- Vinke K, Martin MA, Adams S, Baarsch F, Bondeau A, Coumou D, Donner RV, Menon A, Perrette M, Rehfeld K, Robinson A, Rocha M, Schaeffer M, Schwan S, Serdeczny O, Svirejeva-Hopkins A (2017) Climatic risks and impacts in South Asia: extremes of water scarcity and excess. *Reg Environ Chang* 17:1569–1583. <https://doi.org/10.1007/s10113-015-0924-9>
- Wanders N, Wada Y (2014) Human and climate impacts on the 21st century hydrological drought. *J Hydrol* 526:208–220. <https://doi.org/10.1016/j.jhydrol.2014.10.047>
- Wheeler T, von Braun J (2013) Climate change impacts on global food security. *Science* 341:508–513
- Wijngaard RR, Lutz AF, Nepal S, Khanal S, Pradhananga S, Shrestha AB, Immerzeel WW (2017) Future changes in hydro-climatological extremes in the Upper Indus, Ganges, and Brahmaputra River Basins. *Plos One* 12:e0190224. <https://doi.org/10.1371/journal.pone.0190224>